Available online at www.sciencedirect.com

ScienceDirect

Procedia Structural Integrity 13 (2018) 204–209

Structural Integrity Procedia

www.elsevier.com/locate/procedia

ECF22 - Loading and Environmental effects on Structural Integrity

Grain size influence on fatigue behaviour in a CuZnAl PE SMA

V. Di Cocco[a,*], F. Iacoviello[a], F. Carlino[a], S. Natali[b]

[a] *University of Cassino and southern Lazio, DICeM, via G. Di Biasio 43, 03043, Cassino, FR, Italy*
[b] *University of Rome "Sapienza", DICMA, Via Eudossiana 18, 00184, Rome, Italy*

Abstract

Due to their capability to recover the initial shape, Shape Memory Alloys (SMAs) are widely used in many applications. Different grades are commercially available and they can be classified considering either their chemical compositions (Cu based, Ni based, Fe based and so on..) or according to their mechanical behaviour. The most used SMAs are the Ni based alloys thanks to their performances both in terms of mechanical resistance and in terms of fatigue resistance, but their costs are quite high. Cu based alloys are good competitors of the Ni based alloys. The recent optimization of their chemical composition improved both the corrosion resistance in aggressive environments and their mechanical performances. In this work, the influence of the grain size on fatigue crack propagation in two Cu-Zn-Al SMAs focusing on the damaging micromechanisms.

Keywords: Cu-Zn-Al Shape Memory Alloy; Grain Size; Fatigue Crack Propagation; Microstructure; Damaging micromechanisms

1. Introduction

The ability to recover the initial shape also after high deformation is the main ability of Shape Memory Alloys (SMAs) (Wisutmethangoon et al. (2009)). The SMAs material class is wide, covering Fe-based alloys (i.e. Fe-Pd, Fe-Pt or Fe-Mn-Si), Au based alloys (i.e Au-Cu and Au-Cd), equiatomic and near-equiatomic Ni-Ti alloys (Zhang et al. (2016)) and Cu based alloys (Furlani et al. (2005), Lovey et al. (1999)) as Cu-Zn-Al that have been investigated in this work (Arnaboldi et al. (2011)). The shape memory property characterized by a pseudoelastic effect, is due to a reversible transition from a parent phase (usually named austenite) to a different phase (usually named martensite) without recrystallization due to mechanical loading. Instead, the inverse transformation (from martensite to austenite) is due to the temperature, which must be higher than a critical temperature.

* Corresponding author. Tel.: +39-07762994334; fax: +39-07762993733.
E-mail address: v.dicocco@unicas.it

2452-3216 © 2018 The Authors. Published by Elsevier B.V.
Peer-review under responsibility of the ECF22 organizers.
10.1016/j.prostr.2018.12.034

Nomenclature	
SMA	Shape Memory Alloy
SEM	Scanning Electron Microscope
ry	Yield radius
GN	Grains Number

In the elastic stage three different stages are evident, with a so called "pseudoelastic behaviour" (Fig.1) (Di Cocco et al. (2014)):

1) The first stage is characterized by the linear elastic deformation of the fully austenitic phase;
2) The second stage is quite similar to a plateau: in this stage, the transformation of the austenitic grains into martensite takes place.
3) The third stage is characterized by the linear elastic deformation of the fully transformed martensitic phase.

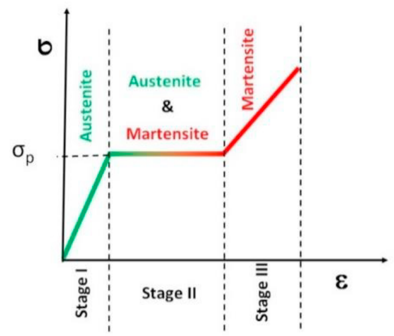

Fig. 1. Schematic representation of a SMA's σ–ε curve (Di Cocco et al. (2014)).

The martensite is obtained from austenite under a loading effect and for this reason is named as "stress induced martensite". The initial shape is obtained recovering the initial austenitic structure, by removing the loads. In this case the stress-strain curve shows a hysteretic behaviour. An elastocaloric cooling effect characterizes the reverse transformation. This is observed in different SMA alloys, as Cu-Zn-Al, Ni-Ti, Ni-Ti-Cu, Ni2FeGa and NiTiHf13.3, with a temperature decrease of about 14°C for Cu-Zn-Al SMA alloy (Iacoviello, et al. (2018)), and it is due to the high values of entropy changing in the reverse transformation.

The studies of Tuma et al. (2016) on a Cu-Al-Ni alloy are focused on the deformation of twinned martensite. It shows the influence of twin spacing (between 10 and 200nm) on energy storage in the alloy, and the importance of the elastic storage energy. Sade et al. (2015) showed the presence in Cu based SMAs of two different martensitic phases (called "18R" and "6R"), evaluating their influence on the cyclic behaviour of a single crystal of SMA, considering the hysteresis phenomenon due to load-unload processes. Policrystalline Cu-Al-Ni SMAs, characterized by a directionally structure due to particular solidification, exhibits an excellent elasticity, and the hysteretic behaviour is reduced when stresses are applied along the grain orientation. These alloys are also characterized by good fatigue resistance and are characterized by less residual strain and slower mechanical properties degradation than commercial NiTi alloys (Fu et al. (2017)).

The Cu-Zn and Cu-Al alloys exhibit a martensitic transformation from cubic β phases, but the first one exhibits the transformation at low temperature (lower than -50°C) and the second one at high temperature (over 100°C). Critical temperature can be changed by adding different elements (the addition of Al in the Cu-Zn alloy allows to obtain a critical temperature below 200°C). The atom diffusion phenomenon governs the transformation, but its kinetic is really slow. For this reason, a cooling process in air allows to obtain a metastable structure that can change under the action of external loads, allowing to change the structure (from austenite to martensite) without recrystallization (Lexcellent et al. (2013)). The transformation from martensite to austenite can take place when:

1) The temperature is higher than the critical temperature (if the critical temperature is lower than environmental temperature, heating is not necessary);
2) The high value loads must be removed.

Large grain sizes Cu-Zn-Al SMAs show that crack paths follow preferentially the grains boundaries (intergranular cracks), sometimes with a propagation that follows a transgranular paths. This is due to the local chemical dis-homogeneities (Natali et al. (2017)). Furthermore in the investigation on the thermodynamic properties of a Cu-Zn-Al SMA, Gomidželović et al. (2015) observed the presence of Zn and Al in the intermetallic phases in polygonal shape grains. In other words, a fine control of the production processes of Cu based alloys could allow to obtain Cu-Zn-Al alloys for different components, ranging from a traditional component obtained from fusion to a complex component made on hybrid composite SMA (Lo Conte et al. (2016). Modern constitutive models are available in the scientific literature (Cisse et al. 2016), covering also microscopic effects as the reorientation of martensite, in order to better describe the behaviour of SMA, not only in terms of stress-strain behaviour, but also in terms of microstructure transformations. In order to improve both the mechanical behavior and the memory performances of Cu based SMA alloys, a grains refinement could be an interesting way. Yang et al. (2016) in Cu-Al-Mn SMA observed an improvement of tensile performances and the damping capability at low temperature and low frequencies by a refinement from 105 μm to 37 μm.

In this work, a Cu-Zn-Al alloy was investigated in order to observe the effects of both the grain sizes on fatigue crack growth propagation. Fracture surfaces were investigated by means of a Scanning Electron Microscope (SEM) in order to identify the main fatigue crack propagation micromechanisms.

2. Investigated alloy and experimental procedure

In this work, the Cu-Zn-Al pseudo-elastic alloy has been investigated considering two different grain sizes and focusing on the fatigue crack propagation resistance.

The SMA alloy characterized by a higher value of grain size (Alloy A – chemical composition in Tab. 1) was produced in the laboratory, by using a controlled atmosphere furnace, and machined in "as cast" conditions.

Table 1: Chemical composition of investigated Cu-Zn-Al alloy (wt%).

Cu	Zn	Al	Other
73.00	21.80	5.04	Bal.

The second investigated alloy (Alloy B) is produced from Alloy A optimizing with the addition of Cerium in order to reduce the grain size. Grain size has been evaluated by means of the LOM (light optical microscope) observations, using Jeffiers method (standard ASTM E883-11) (2017).

In order to evaluate the structure modifications, a customized testing machine equipped with a removable loading frame was used to perform X-Ray analyses at fixed values of applied load and/or deformations. XRD measurements were carried out by using a Philips X-PERT PRO diffractometer equipped with vertical Bragg-Brentano powder goniometer. A step-scan mode was used in the 2θ range from 40° to 45° with a step width of 0.02° and a counting time of 3 s per step (receiving slit 0.02 mm). The employed radiation was monochromated Cu Kα (40kV – 40 mA). The diffractions analyses were performed on a uniaxial specimen both in unloaded and at imposed deformation (ε=10%).

Fatigue crack propagation tests were performed by using the standard CT (Compact Type) specimens obtained by machining the cast ingots. A traditional hydraulic testing machine was used in order to investigate the fatigue crack propagation according to ASTM E 647 (2015).

Fatigue cracks propagation tests were performed according to the following conditions.

- ΔP = constant
- Stress ratio, R = Pmin/Pmax= 0.1
- Loading waveform: Sinusoidal wave.
- Load frequency = 30Hz.
- Testing environment: Lab conditions.

Tests were repeated three times for each investigated condition. Results were characterized by a very high repeatability. Finally, fracture surfaces analyses were performed by means of a Scanning Electron Microscope (SEM) in order to evaluate the influence of grain size, load ratio and applied ΔK on fatigue crack growth micromechanisms.

3. Experimental results and discussion

The minimum grain size has been obtained by means of 0.25wt% of cerium addition, where the initial size of about 150 μm is reduced to 65 μm as shown in Tab 2. The grain size is evaluated by means of planimetric methods (ASTM E 883-11 (2017). It is possible to underline that the main grain size of Alloy A is about double the grain size which characterizes the alloy B. The values of stress plateau for both investigated alloys are shown too.

Table 2: Grain size of investigated alloys and their plateau stresses values σ_p

Alloy	Mean grain size	σ_p [MPa]
A	150 μm	50
B	65 μm	30

Focusing on Alloy B, its microstructure is characterized by the presence of secondary phases at grain boundaries of the larger grains (maybe Cu-Al based and Cu-Zn based alloys (Di Cocco et al. (2014)). This microstructure is often observed in as cast Cu based alloys, and, as a consequence, these alloys usually need a supplementary heat treatment (Yang et al. (2016)). Focusing on Alloy A, the X-ray analysis performed on the as cast unloaded alloy shows a spectrum that exhibits three different peaks corresponding to $2\cdot\theta$ = 43.53°, 40.95° and 43.37°. Corresponding to an engineering deformation ε=10%, the second and third peaks obtained for the unloaded alloy disappear and two new different peaks are present: the first one at $2\cdot\theta$ = 43.57° and the second one at $2\cdot\theta$ = 42.63° (Fig. 2). This implies the microstructure transformation from austenite to stress induced martensite.

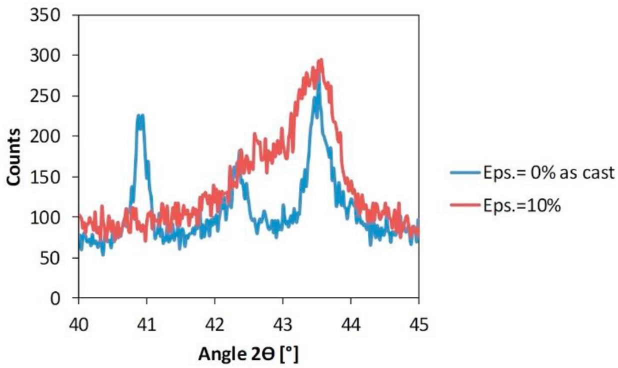

Fig. 2. Spectrum of initial austenite and stress induced martensite (Iacoviello et al. (2018)).

The fatigue crack propagation shows five different stages (Fig. 3), for all the investigated alloys. Considering the Alloy A (Fig. 3a), the first stage ranges between ΔKth=12MPa√m and about 13 MPa√m, and it is followed by a "quasi - plateau" stage (second stage) up to 15 MPa√m. Corresponding to higher ΔK values, a third stage shows an increase of da/dN-ΔK slope up to ΔK =19 MPa√m, followed by a slope decrease of the fourth stage between 19 and 23 MPa√m. Corresponding to higher ΔK values, the fifth stage leads to the instable crack propagation.

An analogous behaviour is observed for the Alloy B, but, in this case, the ranges of the different stages correspond to lower ΔK values (Fig. 3b). In particular, the first stage ranges between the threshold value and 4.5MPa√m and the second stage is almost negligible (between ΔK=5.2 MPa√m and 5.9 MPa√m). This result is confirmed by a previous work (Di Cocco et al. (2014), where a very large grain Cu-Zn-Al SMA showed the presence of five fatigue crack propagation stages in the da/dN-ΔK diagram.

Comparing Alloy A and Alloy B, the second alloy, characterized by lower grain sizes values, is characterized by lower values of the "near – threshold" values and by crack growth rates that are higher by more than a factor of one if compared to the Alloy A, that is characterized by larger grains.

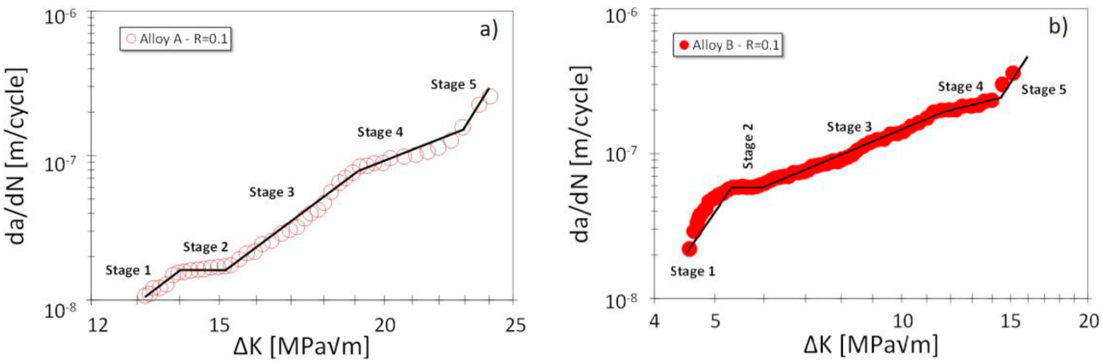

Fig. 3. da/dN-ΔK curves for different grain size: a) grain 150 μm (alloy A), b) grain size 65 μm (alloy B) (Iacoviello et al. (2018)).

Considering the Alloy A, SEM analyses of the fatigue crack surfaces show different crack propagation micromechanisms which characterize the five stages observed. Focusing on Stage 1 fatigue striations are observed with an intergranular crack propagation. Increasing the applied ΔK value, corresponding to stage 2 (Fig. 4a), the crack propagation became mainly transgranular with cleavage morphology, and striations are characterized by increased striation spacing values. Analogous fracture surface morphologies were observed in Alloy B (Fig. 4b).

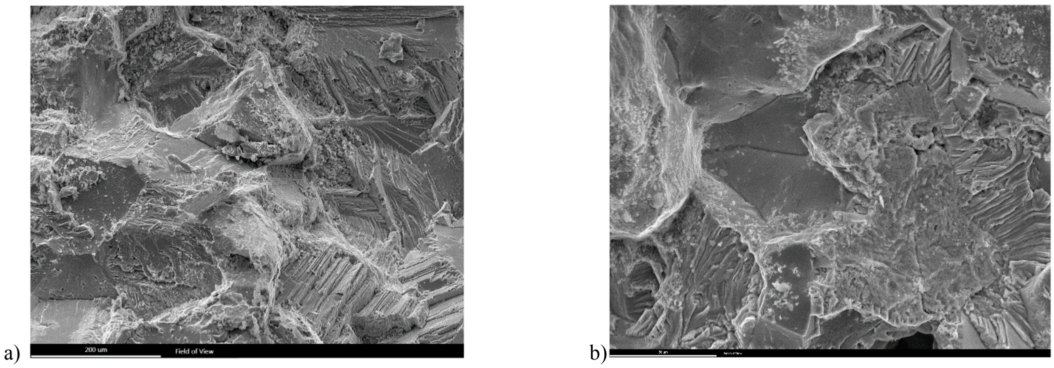

Fig. 4. Stage 2 SEM fracture surfaces observations: a) Alloy A, b) Alloy B.

The second stages are characterized by the presence of a ΔK range with a virtually constant crack growth rate da/dN ("quasi-plateau", e.g. "qp conditions"). Considering that the crack tip plastic radius in homogenous and isotropic materials can be calculated according to Eq. (1)

$$r_y = \frac{1}{2\cdot\pi\cdot}\cdot\left(\frac{K_I}{\sigma_y}\right)^2 \qquad (1)$$

For SMAs it is possible to calculate the radious ahead the crack tip that is interested by a transformation of austenite to martensite (with $K_I = K_{Imax}$) and the fraction of this ratio that is not interested by a reverse transformation for an applied K value equals to K_{min}, considering in Eq. (1) σ_p instead of σ_y and K_{Imin} instead of K_I. Considering the measured grains size in Tab. 2 for the two investigated alloys, the number of grains ahead the crack tip that are interested by a transformation of austenite to stress induced martensite corresponding to K_{Imin} (e.g., GN) can be calculated according to:

$$GN = INT\left[\frac{\frac{1}{2\cdot\pi\cdot}\cdot\left(\frac{K_{Imin}}{\sigma_p}\right)^2}{Grain\ size}\right] \qquad (2)$$

Calculating the GN values for the two investigated alloys, and focusing on K_{Imin} loading conditions, "qp conditions" correspond to about 1 grain for both the investigated alloys (Fig. 5 a and b).

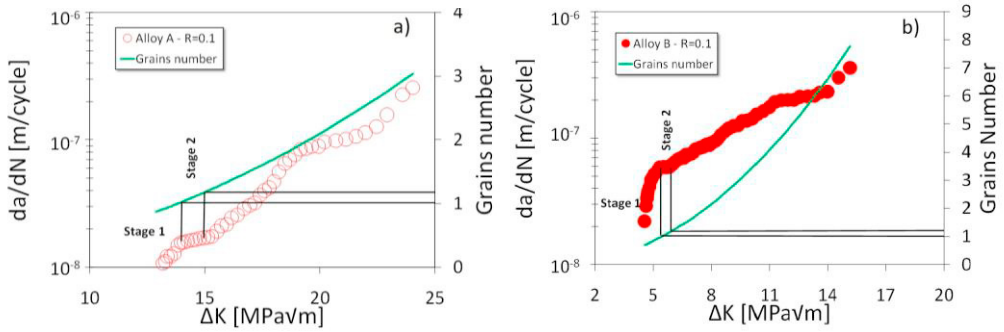

Fig. 5. Grains number corresponding to applied K_{Imin}: a) Alloy A; b) Alloy B

Conclusions

This work is focused on the investigation of the influence of the grains size on the fatigue crack propagation resistance and on the fatigue crack propagation micromechanisms in two Cu-Zn-Al SMAs. Two different SMAs characterized by different grains size were obtained modifying the Ce content. From the metallurgical point of view, the alloy without Ce was characterized by a well developed grain, and the addition of 0.25 wt% of Ce allowed to obtain a reduced grains size, with the presence of intermetallic phases at grains boundaries. From da/dN-ΔK curves, five different stages have been observed. In particular the second stage, characterized by a "quasi plateau" behaviour, is due to the extension of the untransformed field around the crack tip, which is comparable to the grain size.

References

Wisutmethangoon, S., Denmud, N., Sikong, L., 2009. Characteristics and compressive properties of porous NiTi alloy synthesized by SHS technique, Materials Science and Engineering A 515 93–97.

Zhang, X., Wang, S., Yan, X., Yue, D., Sun, R., Zhoue, X., 2016. Probabilistic analysis for the functional and structural fatigue of NiTi wires, Materials and Design 102 213–224.

Furlani, A.M., Stipcich, M., Romero, R., 2005. Phase decomposition in a β Cu–Zn–Al–Ti–B shape memory alloy, Materials Science and Engineering A 392 386–393.

Lovey, F.C., Torra, V., 1999. Shape memory in Cu-based alloys: phenomenological behavior at the mesoscale level and interaction of martensitic transformation with structural defects in Cu-Zn-Al, Progress in Materials Science 44 189-289.

Arnaboldi, S., Bassani, P., Passaretti, F., Redaelli, A., Tuissi, A., 2011. Functional Characterization of Shape Memory CuZnAl Open-Cell Foams by Molten Metal Infiltration, ASM International, JMEPEG20:544–550, DOI: 10.1007/s11665-011-9878-3.

Di Cocco, V., Iacoviello, F., Natali, S., Volpe, V., 2014. Fatigue crack behavior on a Cu-Zn-Al SMA, Frattura ed Integrità Strutturale, 30 454-461; DOI: 10.3221/IGF-ESIS.30.55.

Iacoviello, F., Di Cocco, V., Natali, S., Brotzu, A., 2018. Grain size and loading conditions influence on fatigue crack propagation in a Cu-Zn-Al shape memory alloy, International journal of fatigue, 10.1016/j.ijfatigue.2018.06.039.

Tuma, K., Stupkiewicz, S., 2016. Phase-field study of size-dependent morphology of austenite–twinned martensite interface in CuAlNi, International Journal of Solids and Structures 97–98 89–100.

Sade, M., La Roca, P., De Castro Bubani, F., Lovey, F.C., Torra, V., Yawny, A., 2015. International Conference on Martensitic Transformations, ICOMAT-2014, Materials Today: Proceedings 2S S719 – S722.

Fu, H., Xu, S., Zhao, H., Dong, H., Xie, J., 2017. Cyclic stress-strain response of directionally solidified polycrystalline Cu-Al-Ni shape memory alloys, Journal of Alloys and Compounds 714 154-159, http://dx.doi.org/10.1016/j.jallcom.2017.04.234.

Lexcellent, C., 2013. Shape-memory Alloys Handbook, Wiley, ISBN:978-1-84821-434-7.

Natali, S., Di Cocco, V., Iacoviello, F., D'Agostino, L., Volpe, V., 2017. Crack path and damage in a CuZnAl SMA, Procedia Structural Integrity, 3 217-223, DOI 10.1016/j.prostr.2017.04.049.

Gomidželović, L., Požega, E., Kostov, A., Vuković, N., Krstić, V., Živković, D., Balanović, L., 2015. Thermodynamics and characterization of shape memory Cu−Al−Zn alloys, Trans. Nonferrous Met. Soc. China 252630−2636.

Lo Conte, A., Biffi, C.A., Tuissi, A., Ali, A., 2016. Computational model for delamination growth at SMA-GFRP interface of hybrid composite, 21st European Conference on Fracture, ECF21, 20-24 June 2016, Catania, Italy, Procedia Structural Integrity 2 1538-1545, DOI 10.1016/j.prostr.2016.06.195.

Cisse, C., Zaki, W., Ben Zineb, T., 2016. A review of constitutive models and modeling techniques for shape memory alloys, International Journal of Plasticity 76 244-284.

Yang, J., Wang, Q.Z., Yin, F.X., Cui, C.X., Ji, P.G., Li, B., 2016. Effects of grain refinement on the structure and properties of a CuAlMn shape memory alloy, Materials Science & Engineering A664 215–220.

ASTM E 883-11, 2017. Standard Guide for Reflected–Light Photomicrography.

ASTM E 647, 2015. Standard Test Method for Measurement of Fatigue Crack Growth Rates.